

# Interaction of streamers in air and other oxygen–nitrogen mixtures

A. Luque<sup>1</sup>, U. Ebert<sup>1,2</sup>, and W. Hundsdorfer<sup>1</sup>

<sup>1</sup> *CWI, P.O. Box 94079, 1090 GB Amsterdam, The Netherlands*,

<sup>2</sup> *Dept. Appl. Physics, Eindhoven Univ. Techn., The Netherlands*

(Dated: November 21, 2018)

The interaction of streamers in nitrogen-oxygen mixtures such as air is studied. First, an efficient method for fully three-dimensional streamer simulations in multiprocessor machines is introduced. With its help, we find two competing mechanisms how two adjacent streamers can interact: through electrostatic repulsion and through attraction due to nonlocal photo-ionization. The non-intuitive effects of pressure and of the nitrogen-oxygen ratio are discussed. As photo-ionization is experimentally difficult to access, we finally suggest to measure it indirectly through streamer interactions.

PACS numbers:

Streamer discharges are fundamental building blocks of sparks and lightning in any ionizable matter; they are thin plasma channels that penetrate nonconducting media suddenly exposed to an intense electric field. They propagate by enhancing the electric field at their tip to a level that facilitates an ionization reaction by electron impact [1, 2]. Streamers are also the mechanism underlying sprites [3, 4, 5]; these are large atmospheric discharges above thunderclouds that, despite being tens of kilometers wide and intensely luminous, were not reported until 1990 [6]. Although the investigation of streamers concentrates mainly in gaseous media, they have also been studied in dense matter, such as semiconductors [7] and oil [8]. Streamers have also received attention in the context of Laplacian-driven growth dynamics [9] and a strong analogy with viscous fingering, in particular Hele-Shaw flows [10], has been established.

Both in laboratory [11] and in nature [12], streamers appear frequently in trees or bundles. As their heads carry a substantial net electrical charge of equal polarity that creates the local field enhancement, they clearly must repel each other electrostatically which probably causes the “carrot”-like conical shape of sprites. On the other hand, recent sprite observations [13] as well as streamer experiments ([14], Fig. 7, [11], Fig. 6) also show the opposite: streamers attract each other and coalesce.

Up to now, streamer interactions have not been studied much theoretically, and streamer attraction has not been predicted at all. In coarse grained phenomenological models for a streamer tree as a whole [15], the repulsive electrostatic interaction between streamers is taken into account. In a more microscopic, but still largely simplified model, Naidis [16] studied the corrections to the streamer velocity due to electrostatic interaction with neighboring streamers. In [17], two authors of the present letter have studied a microscopic “fluid” model for a periodic array of negative streamers in two spatial dimensions, where they show that shape, velocity and electrodynamics of an array of streamers substantially differs from those of single streamers due to their electrostatic interaction, but attraction or repulsion were excluded by

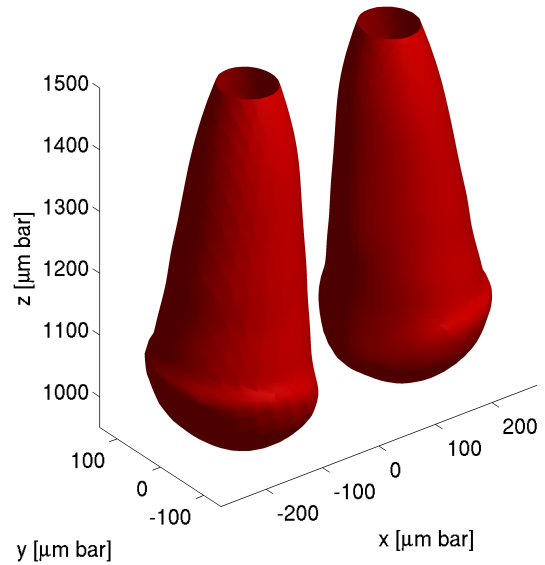


FIG. 1: Two negative streamers in nitrogen at atmospheric pressure advancing downwards and repelling each other; shown are surfaces of constant electron density in an advanced state of evolution within a constant background field. See the text for details.

the approach. Due to the difficulty to represent this multiscale process [2] in a numerically efficient manner, only recently it has become possible to simulate streamers in full 3D [18, 19]. We here present a numerical method to handle this problem, and we apply it to the interaction of streamers in complex gases like air where a nonlocal photon mediated ionization reaction has to be taken into account. We find that when varying gas composition and pressure, streamers can either repel or attract each other. The transition occurs in an unexpected manner, and is not simply determined by an ionization length.

The photon mediated ionization reaction in air and other nitrogen oxygen mixtures is experimentally not easily accessible, but forms a basic ingredient of the present theory of streamers in air [19, 20, 21, 22, 23]; all these simulations are based on the single experimental mea-

surement of Penney and Hummert in 1970 [24]. Our theoretical results suggest that this reaction could be deduced from experiments on coalescence or repulsion of adjacent streamers as a function of pressure and gas composition.

We study the minimal streamer model [25] extended by the nonlocal photo-ionization reaction characteristic for nitrogen oxygen mixtures like air. It consists of continuity equations for electron and ion densities  $n_{e,+}$  coupled to the electrical field  $\mathbf{E}$  that is determined by the potential on the outer boundaries and space charge effects

$$\partial_t n_e = \nabla \cdot (n_e \mu_e \mathbf{E}) + D_e \nabla^2 n_e + S_i + S_{ph}, \quad (1)$$

$$\partial_t n_+ = S_i + S_{ph}, \quad (2)$$

$$\epsilon_0 \nabla \cdot \mathbf{E} = e(n_+ - n_-), \quad \mathbf{E} = -\nabla \phi. \quad (3)$$

Here  $\mu_e$  is the electron mobility,  $D_e$  is the electron diffusion coefficient and  $e$  is the elementary charge. Ion mobility, much smaller than electron mobility, is neglected. To fully focus on the influence of photo-ionization, electron attachment on oxygen is here neglected as well, and we use transport parameters for pure nitrogen as in previous work [2, 26]. The source terms for additional electron-ion pairs are the local impact ionization  $S_i$  in Townsend approximation,  $S_i = n_e \mu_e |\mathbf{E}| \alpha(|\mathbf{E}|) = n_e \mu_e |\mathbf{E}| \alpha_0 e^{-E_0/|\mathbf{E}|}$ , where  $\alpha_0$  is the ionization cross section and  $E_0$  is the threshold field, and the nonlocal photo-ionization according to the model for oxygen-nitrogen mixtures developed by Zhelezniak *et al.* [27]

$$S_{ph}(\mathbf{r}) = \frac{\xi A(p)}{4\pi} \int \frac{h(p|\mathbf{r} - \mathbf{r}'|) S_i(\mathbf{r}') d^3(\mathbf{r}')}{|\mathbf{r} - \mathbf{r}'|^2}, \quad (4)$$

with  $A(p) = p_q/(p + p_q)$ . Here it is assumed that accelerated electrons excite the  $b^1\Pi_u$ ,  $b^1\Sigma_u^+$  and  $c^1\Sigma_u^+$  states of nitrogen by impact with a rate  $\xi S_i$  where  $S_i$  is the local impact ionization rate and  $\xi$  a proportionality factor. These nitrogen states can deexcite under emission of a photon in the wavelength range 980 – 1025 Å that can ionize oxygen molecules [24, 27]. The absorption length of these photons by oxygen is obviously inversely proportional to the oxygen partial pressure  $p_{O_2}$ . Introducing the oxygen concentration in the gas as  $\eta = p_{O_2}/p$ , the absorption function of photoionizing radiation  $h(pr)$  is characterized by the two length scales  $pr_{min} \approx 380 \mu\text{m} \cdot \text{bar}/\eta$  and  $pr_{max} \approx 6.6 \mu\text{m} \cdot \text{bar}/\eta$ . Above a critical gas pressure that we take as  $p_q = 60 \text{ Torr} = 80 \text{ mbar}$  [22], the excited nitrogen states can be quenched by collisions with neutrals, hence suppressing photo-emission; this is taken into account through the prefactor  $A(p)$ .

A major difficulty in the theoretical study of streamer-streamer interactions is the development of an efficient numerical code for streamer simulations with their inner multiscale structure in three dimensions. Here we present a locally adaptive and parallelizable approach to this problem. Our method has in common with the one described in [18] that cylindrical coordinates and a uniform

grid in the angular dimension are used, but in the  $r, z$ -projection we apply the grid refinement scheme of [26] to resolve better the thin, pancake-like shape of the space-charge layer. Furthermore, to allow the parallel solution of the Poisson equation in multi-processor machines we perform a Fourier transformation in the angular coordinate  $\theta$ ,  $\tilde{\phi}_k(r, z) = \sum_{n=0}^{N-1} \phi(r, z, \theta_n) e^{-ik\theta_n}$ , where  $N$  is the number of grid cells in the  $\theta$  direction and  $\theta_n = 2\pi n/N$ . For each separate mode  $k$ , a two-dimensional Helmholtz equation has to be solved:

$$\nabla_{rz}^2 \tilde{\phi}_k + \frac{|w_k|^2}{r^2} \tilde{\phi}_k = -\frac{e}{\epsilon_0} (\tilde{n}_{+k} - \tilde{n}_{ek}), \quad (5)$$

where a tilde  $\tilde{\cdot}$  represents the Fourier transform of a quantity and  $|w_k|^2 = \frac{2}{\Delta\theta^2} (1 - \cos k\Delta\theta)$ . For each Fourier mode, we apply the refinement algorithm described in [28], which is trivially generalized to solve the Helmholtz instead of the Poisson equation. The advantage of solving the electrostatic part of the problem in the Fourier domain is that each of the Fourier modes is decoupled from the rest and hence it can be solved in parallel in a multi-processor computer. Once the electric field is calculated in Fourier space, the field in real space is derived through an inverse Fast Fourier Transform; and the convection-diffusion-reaction system (1)-(2) is integrated as detailed in [26]. The photo-ionization term is computed in a Helmholtz PDE approach as described in [22], and in the angular direction with a scheme of Fourier transformations and parallel solving that is completely equivalent to the one applied to the Poisson equation.

We now use our model and numerical algorithm to study the interaction between two streamers. We focus on the influence of (i) the pressure in air and of (ii) the oxygen-nitrogen ratio at standard pressure; standard temperature is always assumed. (i) The comparison of streamers at different pressures  $p$  relies on scaling lengths, times etc. with appropriate powers of  $p$ . These similarity laws are strictly valid in the minimal streamer model [2, 26]; they are broken by photo-ionization (4) when the pressure reaches the quenching pressure  $p_q$ ; for  $p \gtrsim p_q$ , photo-ionization at unchanged gas composition is increasingly suppressed like  $A(p)$  [20]. Similarity or Townsend scaling is further discussed in Sect. 1.2 of [29]. (ii) The  $\text{O}_2:\text{N}_2$  ratio changes the local photoionization rate which is proportional to it, while the absorption lengths are inversely proportional to it.

First, negative streamers are investigated, because they propagate even in the absence of photo-ionization. Then it is shown that positive streamers behave similarly. In all simulations, we use two identical Gaussian seeds of reduced width (according to Townsend scaling)  $p \cdot w = 73.6 \mu\text{m} \cdot \text{bar}$  and amplitude  $p^{-2} \cdot n_{e,max} = 1.4 \cdot 10^{-2} \mu\text{m}^{-3} \cdot \text{bar}^{-2}$  separated by a reduced distance of  $p \cdot d = 230 \mu\text{m} \cdot \text{bar}$  as an initial condition. They are exposed to a homogeneous and constant background electric field  $E_b/p = 80 \text{ kV}/(\text{cm bar})$  in the positive  $z$  direc-

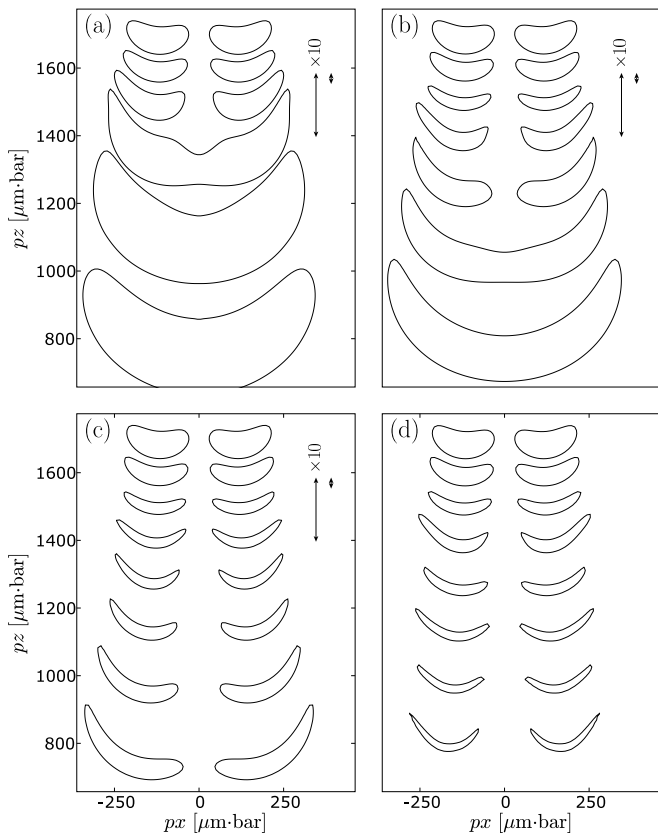


FIG. 2: Evolution of the space charge layers of two adjacent negative streamers at different pressures in air. (a)  $p = 0.07$  mbar, (b)  $p = 1$  bar, (c)  $p = 50$  bar, (d)  $p \rightarrow \infty$ . (a) corresponds to  $A(p) \approx 1$  and (d) to  $A(p) = 0$ , which is equivalent to pure nitrogen since there is no photo-ionization (even though in pure nitrogen the length-scales formally diverge). The axes show reduced lengths  $p \cdot x$ ,  $p \cdot z$  to exhibit similarities. In the upper right corners, the two photo-ionization lengths are inserted as vertical bars. A multiplicative factor is used where the lengths are too long to fit into the figure.

tion. The streamers on reduced length, time and density scales are similar if photo-ionization is neglected.

The simulations were performed with an angular resolution of  $\Delta\theta = 2\pi/64$  ( $N = 64$ ), but we also checked that the results are stable when we double the number of angular grid cells. Figure 1 shows a surface of equal electron density for the discharge in nitrogen at normal pressure and temperature at time  $t = 1.56$  ns. Figures 2-4 show the space charge layers at the streamer heads (more precisely, the half maximum line at the respective time) in the plane intersecting the two streamer axes in timesteps of  $0.12$  ns  $\cdot$  bar; the first snapshot is at time  $0.84$  ns  $\cdot$  bar.

Figure 2 demonstrates the effect of pressure change for similar streamers in artificial air, i.e., in an oxygen nitrogen mixture of ratio 20:80, corresponding to  $\eta = 0.2$ . The panels show (a) air at a pressure of  $0.05$  torr  $\approx 0.07$  mbar, which is the atmospheric pressure at approximately 70 km height, where sprites are

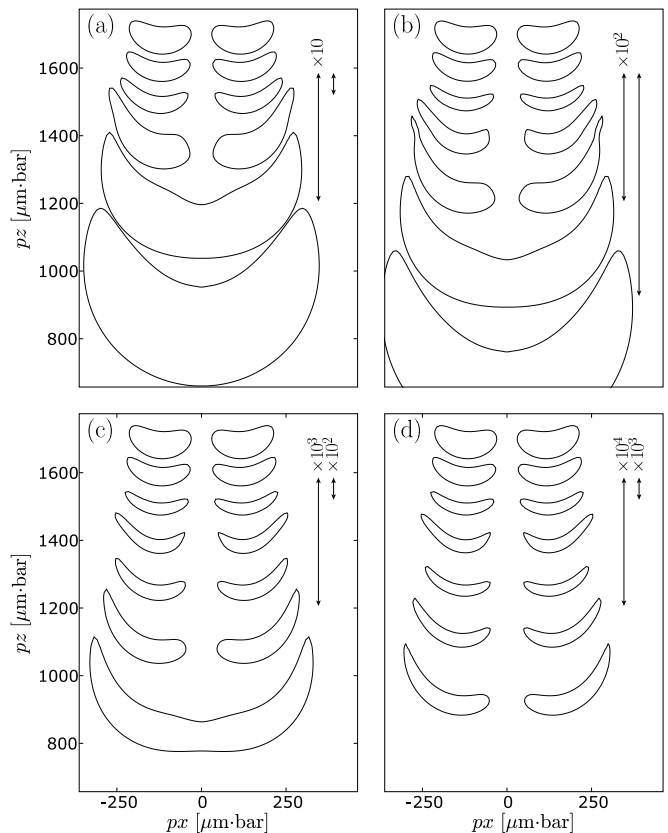


FIG. 3: Evolution of the space charge layers of two adjacent streamers at atmospheric pressure, but different concentrations of  $O_2$ :  $\eta = p_{O_2}/p = 10^{-1}$ ,  $10^{-2}$ ,  $10^{-3}$ ,  $10^{-4}$  in panels (a)–(d). The two photo-ionization lengths are again inserted as vertical bars in the upper right corners.

frequently observed, (b) air at 1 bar, (c) air at 50 bar, and (d) pure nitrogen which in our model is equivalent to air at infinite pressure.

The first observation is that two streamers do not always repel each other. Rather there are two qualitatively different regimes: at a pressure of 50 bar and above, when the fast collisional quenching of  $N_2$  molecules suppresses photoionization, the streamers repel each other electrostatically due to the net negative charge in their heads. However, at atmospheric pressure and below, the streamers attract each other: a cloud of electrons is created between the two streamers which eventually makes them coalesce into a single, wider one. As it has been suggested that the photo-ionization length could determine length scales in the streamer head [30], the two reduced photoionization lengths are indicated by the vertical bars in the upper right corners, they are the same in all panels. Obviously, there is no simple relation between these lengths and the observed repulsion or attraction; the interaction is rather governed by the quenching prefactor  $A(p)$ .

Figure 3 demonstrates the effect of the oxygen concentration. For fixed atmospheric pressure, the rel-

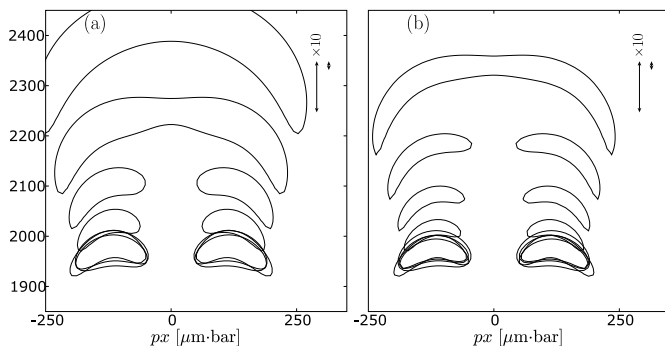


FIG. 4: Evolution of the space charge layers of two adjacent positive streamers in air at atmospheric pressure at 1 bar (a) and 50 bar (b).

ative oxygen concentration  $\eta = p_{O_2}/p$  is reduced to  $10^{-1}$ ,  $10^{-2}$ ,  $10^{-3}$ ,  $10^{-4}$  in panels (a)–(d). As the photoionization lengths scale inversely with the oxygen concentration, these lengths increase by factors 10 from one panel to the next while the prefactor decreases with a factor  $10^{-1}$ . The attraction between the streamers decreases with decreasing oxygen concentration until it is not visible anymore in panel (d) for  $\eta = 10^{-4}$ .

Figure 4 shows that the interaction between two positive streamers is qualitatively similar to that of two negative streamers, since the same two competing phenomena are present. Initial and boundary conditions are the same, and panels (a) and (b) show positive streamers in air at atmospheric pressure and at 50 bar. The positive streamers take longer to start but after a relatively short time they merge.

Due to the nonlinear and nonlocal nature of streamer interactions and to the many dimensions of our parameter space, it is difficult to develop a simple prediction for streamer merging. Nevertheless, the following remarks can be made. First, to produce enough ionization between the streamers, at least one of the absorption lengths of photo-ionization must be larger than or comparable to the streamer distance. Second, this photo-ionization is only amplified to a level comparable to that on the streamer head if the field is enhanced between the streamers; hence the streamer distance should not be much larger than the streamer radius. Finally, an approximation for the relative photo-ionization level can be extracted from (4) as the maximum of the instantaneous rate of photo-ionization on the middle axis produced per impact ionization event in the tip of a given streamer, namely  $\beta = \xi A(p)h(pd/2)/\pi p^2 d^2$ . Preliminary results show that this parameter influences the electron densities in the axis at early stages of the evolution. We have not found a deterministic law but coalescence is favoured for large  $\beta$  and occurs always if  $\beta \gtrsim 10^{-11} \mu\text{m}^{-3} \cdot \text{bar}^{-3}$ .

We have developed a code to study the interaction of streamers in full 3D space, and we have studied the ba-

sic processes that govern the interaction of two adjacent streamers. To focus on the underlying physics of photoionization we have neglected electron attachment and nontrivial electrode geometries. Further steps are needed to successfully predict the outcome of experiments and observations; we mention needle electrodes and the non-alignment of the streamer heads. But our results show that for a given pressure  $p$ , electric field  $E_0$ , oxygen-nitrogen ratio  $\eta$  and initial seeds, there is a threshold distance  $d^*$  below which two streamers coalesce. This distance, which is experimentally accessible, would be an indirect measure of the frequency of photoionizing events. Hence we believe that fully three-dimensional calculations of streamer dynamics will provide a suitable test-case for streamer models as they predict easily observable behavior like attraction, repulsion or branching.

A.L. acknowledges support by Netherland's STW project 06501. U.E. and W.H. acknowledge support by the Dutch national program BSIK, in the ICT project BRICKS, theme MSV1.

- 
- [1] Y. P. Raizer, *Gas Discharge Physics* (Springer, Berlin, 1991).
  - [2] U. Ebert *et al.*, *Plasma Sour. Sci. Tech.* **15**, S118 (2006).
  - [3] H. C. Stenbaek-Nielsen *et al.*, *Geophys. Res. Lett.* **34**, 11105 (2007).
  - [4] V. Pasko *et al.*, *Geophys. Res. Lett.* **25**, 2123 (1998).
  - [5] V. P. Pasko, in *Sprites, Elves and Intense Lightning Discharges*, ed.: M. Füllekrug *et al.*, (Springer Netherlands, 2006), pp. 253–311.
  - [6] R. Franz *et al.*, *Science* **249**, 48 (1990).
  - [7] P. Rodin, I. Grekhov, *App. Phys. Lett.* **86**, 243504 (2005).
  - [8] G. Massala and O. Lesaint, *J. Phys. D* **34**, 1525 (2001).
  - [9] M. Arrayás *et al.*, *Phys. Rev. Lett.* **88**, 174502 (2002).
  - [10] B. Meulenbroek *et al.*, *Phys. Rev. Lett.* **95**, 195004 (2005).
  - [11] T.M.P. Briels *et al.*, *J. Phys. D* **39**, 5201 (2006).
  - [12] E. Gerken *et al.*, *Geophys. Res. Lett.* **27**, 2637 (2000).
  - [13] S. A. Cummer *et al.*, *Geophys. Res. Lett.* **33**, 4104 (2006).
  - [14] G. Winands, *et al.*, *J. Phys. D* **39**, 3010 (2006).
  - [15] M. Akyuz, *et al.*, *J. Electrostatics* **59**, 115 (2003).
  - [16] G. V. Naidis, *J. Phys. D: Appl. Phys.* **29**, 779 (1996).
  - [17] A. Luque, F. Brau, U. Ebert, arXiv:0708.1722.
  - [18] A. A. Kulikovskiy, *Phys. Lett. A* **245**, 445 (1998).
  - [19] S. Pancheshnyi, *Plasma Sour. Sci. Tech.* **14**, 645 (2005).
  - [20] N. Liu, V. P. Pasko, *J. Phys. D* **39**, 327 (2006).
  - [21] P. Ségur *et al.*, *Plasma Sour. Sci. Tech.* **15**, 648 (2006).
  - [22] A. Luque *et al.*, *App. Phys. Lett.* **90**, 081501 (2007).
  - [23] A. Bourdon *et al.*, *Plasma Sour. Sci. Tech.* **16**, 656 (2007).
  - [24] G. Penney, G. Hummert, *J. Appl. Phys.* **41**, 572 (1970).
  - [25] P. Vitello *et al.*, *Phys. Rev. E* **49**, 5574 (1994).
  - [26] C. Montijn *et al.*, *J. Comput. Phys.* **219**, 801 (2006).
  - [27] M. Zheleznyak *et al.*, *High Temp.* **20**, 357 (1982).
  - [28] J. Wackers, *J. Comp. Appl. Math.* **180**, 1 (2005).
  - [29] T.M.P. Briels, E.M. van Veldhuizen, U. Ebert, arXiv:0805.1364.
  - [30] A. Kulikovskiy, *J. Phys. D* **33**, 1514 (2000).